Smart Coordination Schemes for Multiple Battery Energy Storage Systems for Support in Distribution Networks with High Penetration of Photovoltaics

IET Smart Grid

Special Section: Selected Papers from the 7th IET Renewable Power Generation Conference (RPG 2018)

IET Journals
The Institution of Engineering and Technology

Smart coordination schemes for multiple battery energy storage systems for support in distribution networks with high penetration of photovoltaics

eISSN 2515-2947
Received on 22nd March 2019
Revised 6th August 2019
Accepted on 7th August 2019
E-First on 2nd September 2019
doi: 10.1049/iet-stg.2019.0094
www.ietdl.org

Obinna Unigwe[1] ✉, Dahunsi Okekunle[1], Aristides Kiprakis[1]

[1]*School of Engineering, The University of Edinburgh, The King's Building, EH9 3DW, Edinburgh, UK*

✉ *E-mail: o.unigwe@ed.ac.uk*

Abstract: The use of battery energy storage system (BESS) is one of the methods employed in solving the major challenge of overvoltage, experienced on distribution networks with high penetration of photovoltaics (PV). The overvoltage problem limits the penetration levels of PV into the distribution network, and the benefits that could be gained. This study presents three loosely-related schemes for the coordination of multiple BESSs in such networks. Through the efficient selection, coordination and timing of charge and discharge operations of the BESS, the scheme maintains bus voltages within statutory ranges during periods of high PV power generation and high network load demand. Network segmentation was used in two of the schemes to encourage more even utilisation of the BESS in order to maximise the economic benefits of the BESS. The algorithms for the schemes were implemented and demonstrated on two different distribution networks. Simulation results showed that the schemes met the objectives of mitigating overvoltage and more even cycling of the BESSs during their operating lifetimes.

1 Introduction

The electricity network is currently undergoing transformative changes globally, as it transits from the more traditional structures that involve unidirectional power flow from large generating plants, often fossil fuel-powered, into more flexible structures. The new structures accommodate multidirectional power flows, newer renewable energy sources (RES) and other low carbon technologies. Of the RES, the photovoltaic (PV) has experienced the highest capacity of installations in the last decade [1]. A challenge with the transition from classical to so-called 'smart grid' is that the grid was not originally designed with these changes in mind. The consequence of this is that technical complications arise, that must be dealt with, in the presence of increasing penetration of RES. Power quality issues such as harmonics, reverse power flow, voltage unbalance and overvoltage are common. Overvoltage, in particular, constitutes a major limitation to higher penetrations of PV in the network, especially because there are many periods with substantially higher PV generation levels when compared to consumption on the network.

Methods such as curtailment, use of reactive power injection and absorption, on-load tap changer operations and battery energy storage system (BESS) have been employed to solve these technical challenges [2]. BESSs have grown in popularity for use in stationary applications in electric network systems. Reasons for the increasing widespread deployment of BESS include flexibility and speed in dispatch of active (sometimes reactive) power when required [3]. Falling costs of BESS also account, in part, for the growth in popularity of BESS use in power systems applications. High interest and demand for batteries for use in consumer electronics and transport have motivated increased investment, research and development in the manufacture of cheaper and more efficient batteries [4]. Battery prices are expected to continue falling in the coming years [5].

This favourable trend on battery prices notwithstanding, BESS is still acquired at significant costs in the present, and therefore, justification for such investments becomes necessary. On the other hand, it has been established that the method and manner of operation of BESS have a significant impact on the lifespan of BESS [6]. It then follows that there is a need for highly efficient coordination of operations of installed BESSs on the network, to maximise the economic benefits, while meeting the specific objectives of installation.

A number of studies have been carried out to improve the operations of BESS in power networks. In [7], a rule-based strategy was presented for the charging/discharging of BESSs that are co-located with rooftop PVs. The focus was on calculating charge/discharge rates that maintain the state of charge (SOC) of the batteries within range for overvoltage mitigation and peak support in the evening. This paper, however, did not consider the potential uneven cycling of BESSs placed at different locations. In [8–11], methods of operation of BESS in power networks were examined for varying objectives. A control algorithm for mitigating frequency and voltage deviations was presented in [12], but this strategy did not consider the effects of daily cycling, and therefore techno-economic justification for installation will be difficult. In [13], a coordination algorithm for control of multiple BESSs was carried out based on voltage sensitivity. Considerations were made to achieve evenly-spread participation of BESSs over time, but this paper did not consider the decrease in sensitivity/impact of the BESS as electrical distance from target bus increases. In [14], a dispatch control strategy for BESS was developed using stochastic programming. The work also involved a ranking order for ensuring even utilisation of BESS across lifetimes – from which some parts have been adopted in our work [14], however did not consider the reduced impact of the BESS active power as the distance increases.

This paper presents three schemes that coordinate the operations of multiple BESSs installed on a network. The objectives of the schemes are to ensure that BESSs are operated in ways that meet the technical objectives of installation while ensuring they are cycled in manner favourable to the health and long life of the BESSs. The schemes are presented with their methods and considerations, followed by simulations and analysis of performances. This work is an expansion of the earlier work carried out in [15].

The rest of the paper is organised as follows. Section 2 presents a description of the problem while Section 3 presents the flat structure sensitivity scheme (FSSS). Section 4 presents the uniform neighbourhood participation scheme (UNPS) while Section 5 has the rotational neighbourhood participation scheme (RNPS). Section

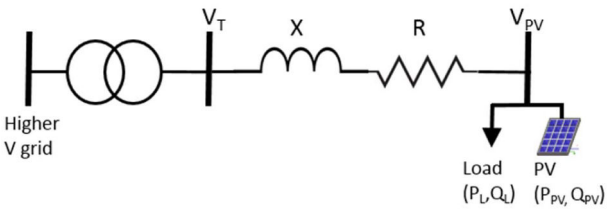

Fig. 1 *Simple radial network with distributed generator*

6 presents the implementation and simulation results of the schemes and finally, conclusion is drawn in Section 7.

2 Problem description and BESS characteristics

Typical radial networks with no distributed generation (DG) along the feeders have unidirectional power flow from the substation down to the end of the feeder. For such networks, voltage magnitudes also decrease from the substation down along the feeder. With the introduction of DG such as PV, the feeder voltage behaviour changes. Consider the simple network depicted in Fig. 1.

The network consists of the substation and power line connecting the substation to the load. On the same bus as the load is connected a PV generator. An expression for the voltage across the network with respect to the buses is given as

$$V_{\mathrm{PV}} - V_{\mathrm{T}} = \Delta V = \frac{R(P_{\mathrm{PV}} - P_{\mathrm{L}}) + X(Q_{\mathrm{PV}} - Q_{\mathrm{L}})}{V_{\mathrm{PV}}} \tag{1}$$

where R and X are the resistance and reactance of the line, respectively. P_{PV} and Q_{PV} are the active and reactive power of the PV generation, V_{T} and V_{PV} are the voltages at the substation and the bus of PV connection, respectively, while P_{L} and Q_{L} are the load active and reactive powers. In the event of $P_{\mathrm{PV}} > P_{\mathrm{L}}$, voltage rise along the feeder may be experienced and thus violating statutory voltage thresholds for operation on the network. Other impacts of high PV penetration are investigated in the work done in [16]. Continued violation of these thresholds could lead to disconnection of the distributed generators from the network [17]. Reducing the resistance and reactance of the lines is one way to solve this problem, as seen in (1). This can be done by replacing existing lines with larger diameter lines, but this usually comes at high costs. Another solution is increasing the P_{L} and Q_{L} and this can be achieved by adding BESS to the network. Due to the dispatchable nature of the BESS, loading on the network can be controlled at different times as required, and network constraint violations can be mitigated. For networks with multiple BESS installations, there arises, therefore, the challenge of coordination of operations of the BESS in such a way that lifespans of the BESSs are preserved for economic reasons, while satisfying the technical objectives of installation.

2.1 BESS characteristics

The state of energy in the battery at any instant in time $E_{\mathrm{BESS}}(t)$ is determined by the change in energy from the previous time instant, given as

$$\Delta E_{\mathrm{BESS}} = E_{\mathrm{BESS}}(t) - E_{\mathrm{BESS}}(t-1) \tag{2}$$

The change in energy is dependent on the charge/discharge power of the BESS, expressed as

$$P_{\mathrm{B}}(t) = \begin{cases} \dfrac{\Delta E_{\mathrm{BESS}}}{\Delta t} \cdot \eta_{\mathrm{c}}^{-1}, & P_{\mathrm{B}}(t) > 1 \\ \dfrac{\Delta E_{\mathrm{BESS}}}{\Delta t} \cdot \eta_{\mathrm{d}}, & P_{\mathrm{B}}(t) < 1 \end{cases} \tag{3}$$

where $P_{\mathrm{BESS}}(t)$ is the charge or discharge power of BESS (positive for charging and negative for discharging), and Δt is the sampling or operation interval, η_{d} is the discharge efficiency and η_{c} is the charge efficiency [18]. Constraint on the depth of discharge (DOD) of the BESS is given as

$$\mathrm{SOC}_{\min} . \quad \leq \mathrm{SOC} \leq \mathrm{SOC}_{\max} . \tag{4}$$

$\mathrm{SOC}_{\min}$. and $\mathrm{SOC}_{\max}$. are the minimum and maximum SOC of the BESS. Idling losses in the BESS are considered to be negligible in this work. Equations (2), (3) and constraint (4) describe the behaviour of the battery model used in this work. This model has been chosen because it captures the characteristics of the battery that are of interest.

3 Flat structure sensitivity scheme

For multiple BESSs connected in a network, a major objective of the coordination scheme is to resolve the challenge of BESS selection for operations at different times for different network conditions, and also the determination of how the selected BESS behaves – charge/discharge rates and DOD. The FSSS utilises the voltage sensitivities of the network nodes to coordinate the operations of participating BESSs, in a way that considers the entire network as a flat non-hierarchical and non-segmented structure. The method of derivation and use of voltage sensitivity, including the operational principles of the flat-structure scheme are presented in this section.

3.1 Voltage sensitivity for BESS selection

The relationship between the changes in voltage at the buses, as a consequence of the changes in active or reactive power at other buses on the network is provided by the voltage sensitivity factor. The Jacobian matrix in (5) presents this relationship

$$\begin{bmatrix} \Delta\theta \\ \Delta|V| \end{bmatrix} = J^{-1} \begin{bmatrix} \Delta P \\ \Delta Q \end{bmatrix} \tag{5}$$

where

$$J = \begin{bmatrix} \dfrac{\delta P}{\delta \theta} & \dfrac{\delta P}{\delta V} \\ \dfrac{\delta Q}{\delta \theta} & \dfrac{\delta Q}{\delta V} \end{bmatrix} \tag{6}$$

In this equation, $\Delta\theta$ is the change in bus voltage angle, ΔQ is the change in reactive power, ΔV is the change in bus voltage and ΔP is the change in active power. Equations (5) and (6) present equations for sensitivities of both voltage angle and magnitude. Of particular interest to this work is ΔV and this is expressed as

$$\Delta|V| = \begin{bmatrix} \dfrac{\delta V}{\delta P} & \dfrac{\delta V}{\delta Q} \end{bmatrix} \cdot \begin{bmatrix} \Delta P \\ \Delta Q \end{bmatrix} \tag{7}$$

Under network conditions of overvoltage, undervoltage and during periods where peak shaving is required, the voltage sensitivity is utilised in the appointment of BESS and determination of charge and discharge rates. In this scheme, in relation to (7), ΔP represents the charge or discharge power of the operational BESS, which can be converted to respective charge/discharge rates, while ΔV is considered at the node where the voltage change is desired. This method of selection ensures that the selected BESS has the most effective desired effect on the voltage of the target node.

A drawback of using the Jacobian matrix method for obtaining voltage sensitivity is the computational complexity that is involved in the process. A method of sensitivity evaluation was presented in [19], and this method provides an alternative computationally less intense way of obtaining the sensitivity matrix. The method is an approximate evaluation, however, the results obtained are close to those obtained by using (1) directly. This method is summarised as follows:

$$\frac{\delta E_i}{\delta P_j} = -\frac{1}{E_n}\left[\sum_{hk \in PT_{i,j}} R_{hk}\right] \tag{8}$$

$$\frac{\delta E_i}{\delta Q_j} = -\frac{1}{E_n}\left[\sum_{hk \in PT_{i,j}} X_{hk}\right] \tag{9}$$

R_{hk} and X_{hk} are the resistance and reactance of branch hk, respectively; E_n is the approximate rated voltage of the network; $PT_{i,j}$ is the set of nodes contained in the path connecting the medium voltage (MV) busbar to nodes i and j, and at the same time common to both nodes.

Sensitivity ranking tables B_P and B_Q for real and reactive power, respectively, are formed using (8) and (9). Only B_P is shown, since this work considers only active power changes, but the formation of B_Q is in a similar fashion to B_P

$$B_P = \begin{bmatrix} \frac{\delta E_1}{\delta P_1}\Delta P_1 & \dots & \dots & \frac{\delta E_1}{\delta P_N}\Delta P_N \\ \dots & \dots & \dots & \dots \\ \dots & \dots & \dots & \dots \\ \frac{\delta E_N}{\delta P_1}\Delta P_1 & \dots & \dots & \frac{\delta E_N}{\delta P_N}\Delta P_N \end{bmatrix} \tag{10}$$

N represents the total number of buses on the network and $n = 1, 2...N$ represents any specific bus on the network. The rows represent the node voltages and the columns represent the BESS locations. When the voltage of a particular bus (along rows) is of interest for change, the column (representing BESS installation location) with the highest value is selected as the best suited for affecting the required voltage change. This selected BESS is designated BESS_{sel} for the time instant that this evaluation is carried out. The selection according to ranking is carried out by the selection evaluator (SE) within the algorithm. When there is no BESS installation on a particular bus, the position of that bus in (10) is set to zero and therefore cannot be selected.

3.2 Description of sets used in formulation

The algorithm, during operation, maintains and updates the following sets at each time step.

3.2.1 Power rating set (P_{BES}): This is the set of active power ratings of all BESSs on the network

$$P_{\text{BES}} = \{P_{\text{BES}_n} : n = 1, 2, \dots, N\} \tag{11}$$

where P_{BES_n} is the active power rating of the BESS connected to bus n, N is the total number of buses on the network. Observe that $P_{\text{BES}_n} = 0,\ \forall n \in Z$ holds true, where Z is the set of all buses that have no BESS installation.

3.2.2 Selected BESS set (BES_{sel}): This is the set of all BESSs that have been selected by the SE and activated for charging or discharging

$$\text{BES}_{\text{sel}} = \{\text{BES}_{\text{sel}_n} : n = 1, 2, \dots, N\} \tag{12}$$

where $\text{BES}_{\text{sel}_n}$ is an output from the SE which denotes the BESS that has been selected for charging. $\text{BES}_{\text{sel}} = \varnothing$ holds true as an initial condition at the start of operations. $\text{BESS}_{\text{sel}_l}$ is used to denote the last BESS that has been added to BES_{sel}.

3.2.3 Charge rates set (CR): This is a set of the charge or discharge rates of corresponding selected BESS contained in BES_{sel}

$$\text{CR} = \{\text{CR}_n : n = 1, 2, \dots, N\} \tag{13}$$

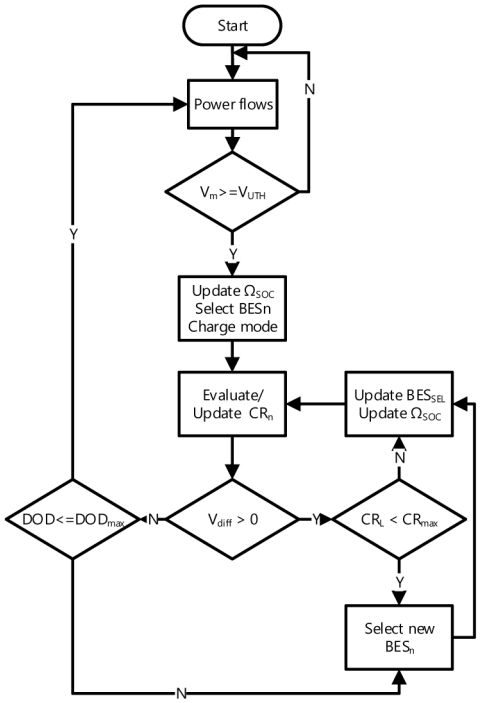

Fig. 2 *Flowchart of coordination scheme (overvoltage)*

where CR_n is the charge rate of the corresponding $\text{BES}_{\text{sel}_n}$. Similar to BES_{sel}, $\text{CR} = \varnothing$ holds true at the start of operations. CR_l is used to denote the charge rate of $\text{BES}_{\text{sel}_l}$ and CR_{max} denotes the maximum charge rate of any BESS.

3.2.4 State of charge set (Ω_{soc}): This set contains the changing SOC of all the BESSs on the network. The algorithm uses this to have knowledge of which BESS are fully charged, or nearly fully charged in order to take proactive actions. The latter is one of the objectives the scheme aims to achieve.

3.3 FSSS operation

The flowchart in Fig. 2 shows the operation of the FSSS. In this work, the algorithm coordinates multiple BESS on a network with the objectives of mitigating overvoltage during periods of high PV generation and mitigating undervoltage during high loading periods. High loading periods often coincide with periods of low PV generation, usually in the evening. The bus voltages are maintained within set upper and lower limits, $V_{\text{LTH}} \le V_{\text{m}} \le V_{\text{UTH}}$. V_{m} is the monitored bus voltage, V_{LTH} is the statutory lower threshold voltage and V_{UTH} is the statutory upper threshold voltage. Fig. 2 shows the scheme for overvoltage alone, but the same flow of controls applies for undervoltage situations, with the BESS discharging instead of charging.

Following a scenario where the algorithm is initialised at the start of the day (midnight), then $V_{\text{m}} > V_{\text{UTH}}$ is likely to occur first as a result of possible overvoltage due to high PV power generation in the day when load demand is low. Upon overvoltage, the SE executes the evaluation and the output from the SE is $\text{BES}_{\text{sel}_n}$, and this BESS goes into charging mode. V_{diff} is the difference between the measured bus voltage V_{m} and the statutory threshold voltage V_{UTH} or V_{LTH}. CR_n, which is the amount of power that keeps V_{diff} at zero, is also derived for $\text{BES}_{\text{sel}_n}$. CR_n is calculated as shown in (14), which is derived from (10)

$$\text{CR}_n = V_{\text{diff}} \cdot \left(\frac{\delta V_{\text{m}}}{\delta P_n}\right)^{-1} \tag{14}$$

$(\delta V_{\text{m}}/\delta P_n)$ is the sensitivity V_{m} to the bus where $\text{BES}_{\text{sel}_n}$ is connected. During operation, given the situation where the CR of $\text{BES}_{\text{sel}_n}$ stops being large enough to maintain $V_{\text{diff}} = 0$, possibly as

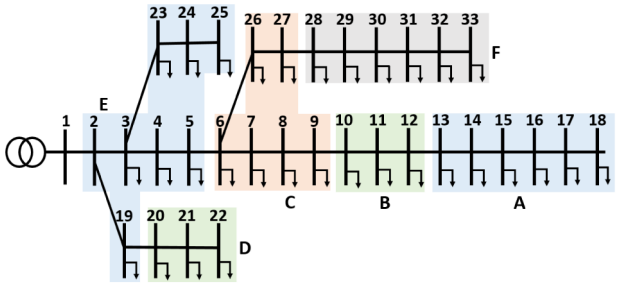

Fig. 3 *IEEE 33-bus distribution network*

a result of sustained increase in PV active power generation, new BESS are added, one at a time, to the BES_{sel} set. The selection this time will exclude from the ranking, any BESS that is already contained in BES_{sel}.

The SOC of participating BESSs is known since Ω_{SOC} is updated at every time step. With this information, new BESS are added to the BES_{sel} set just before any active BESS is charged or discharged to the maximum or minimum SOC, mitigating any unwanted voltage changes that could occur.

The BESS enters discharge mode anytime during operations that the condition $V_m < V_{LTH}$ is satisfied, or at set times for shaving operations during periods of high load demands. A similar procedure to charge operations is followed for the discharge operations. V_{UTH} is replaced by V_{LTH} in the algorithm for the evaluation of V_{diff}, causing V_{diff} to return negative values, and consequently negative values of CR_n. Negative CR_n values represent discharge signals to the BESS.

4 Uniform neighbourhood participation scheme

The cost of BESS is the major limitation to increased installations on power networks. It then becomes necessary that initial cost of installation be justified, as well as delaying, as much as possible, any future replacement costs. As the length of life of the battery is a function of the way it is operated during its lifetime, it then follows that the systematic operation in a manner to promote good health and prolong the lifetime, while satisfying the technical aims of installation of BESS, is an important objective.

One common scenario encountered in networks with BESS installations is where, due to network topology and structure, BESS connected to certain buses end up being cycled more frequently than others, as a result of their locations. Such BESS therefore reaches end-of-life quicker, thereby subjecting owners and operators to replacement costs, while some other BESS are not being put to use as much. Such replacements do not benefit from the advantages of economy of scale, among other undesirable consequences. The challenge encountered in the scenario, as described, and other cases that lead to wildly disproportionate cycling across multiple BESS in the same network, is what the UNPS aims to overcome.

In this scheme, the network is segmented into BESS operational zones. The BESSs in each zone operate in a cooperative and uniform manner to respond to events within the zone with charge and discharge operations as required. The sensitivity method introduced in Section 3 is applied to determine the charge and discharge rates of the BESS for any active zone. A zone becomes active when the voltage on any bus in the zone exceeds the defined thresholds. This means that more than one zone can be active at any time. Zonal neighbours (ZN) are zones configured with ability to respond to distress signals from each other, when the source zone for the distress is unable to sufficiently deal with the undesirable event. Every zone therefore possesses a hierarchical set, Z_{nbr}, that contains a list of every zone that it shares zonal neighbourhood with. The hierarchical structure of Z_{nbr} means that the first zone in the set is given priority appointment to attempt to resolve the distress. Only after the first element in Z_{nbr} is unable to resolve the problem is the second zone appointed, then the third, and so on. For example, the zonal neighbourhood set for zone B in a network is given as.

$$Z_{nbr|B} = [D, C, A, E] \tag{15}$$

Zone D is the priority zone to respond to distress signals from zone B when the BESSs in zone B are not sufficient to resolve the problem, followed by zone C and then zone E.

4.1 Network segmentation considerations

The segmentation of the network into zones for the implementation of the neighbourhood scheme considers a number of factors peculiar to the network. The first consideration is the electrical distances between the buses. With the increase in the length of the lines between buses comes a corresponding increase in the resistance between them.

The sensitivity values for buses electrically closer to each other are higher than that for buses that are farther apart, and therefore can more easily affect the voltages of each other. When using BESS active power for voltage control in the neighbourhood scheme, the aim therefore is to minimise the distances between the participating BESS in each zone. Areas of the network with shorter line distances apart are likely to be placed in the same zone while longer line distances are likely to form inter-zone boundaries. For implementation of the ZN feature, zones with shorter inter-zonal distances are likely to belong to the same zonal neighbourhoods. Segmentation of the test network used to demonstrate the scheme is shown in Fig. 3.

4.2 Operation of the UNPS

Let the network be segmented into Φ zones, where $\Phi = A, B, C\ldots$. Each zone can contain any number of BESS, depending on unique network features considered during segmentation, described in Section 4.1. Let the number of BESS in each zone be $1, 2, 3\ldots K$, so that if zones A and B, for example, have four and five BESS, respectively, the zones will be

$$\begin{aligned} A &= [A1,\ A2,\ A3,\ A4]; \\ B &= [B1,\ B2,\ B3,\ B4,\ B5] \end{aligned} \tag{16}$$

Z_{sel} is a set of all active zones and is updated at every time step of operations.

The scheme switches the BESSs into charge or discharge operation mode for any zone when the condition $V_{LTH} \le V_m \le V_{UTH}$ ceases to remain true for any bus in the zone. This means overvoltage or undervoltage on a single bus switches all the BESS in the zone from where the signal was sent. The BESS charge and discharge rates change in a uniform fashion until the distress signal discontinues.

The algorithm also updates the Z_{nbr} for each zone according to availability at any given time. The Z_{nbr} is used when distress signal persists in an operational zone, even when all the participating BESS in the operational zone are charging or discharging at maximum possible rates. When this happens, the first zone in Z_{nbr} for the zone in question is checked for availability and then appointed if available. If unavailable, the second zone in Z_{nbr} is checked, and so on. The newly-appointed zone is added into the Z_{sel} set. The zone goes into operation, despite the condition $V_{LTH} \le V_m \le V_{UTH}$ not violated on any of the buses in its zone.

5 Rotational neighbourhood participation scheme

The RNPS is a hybrid combination of the FSSS and UNPS. Like the UNPS, the segmentation of the network into zones, described in Section 4.1 is maintained; and like the FSSS, within each active zone, the BESSs charge and discharge in turns and not uniformly. Section 5.1 describes other features and operations of the RNPS.

5.1 Operation of the RNPS

In the RNPS, BESSs in each zone also belong to the same neighbourhood and only respond to events within the zones, except in cases where the Z_{nbr} is used to appoint a neighbour zone when

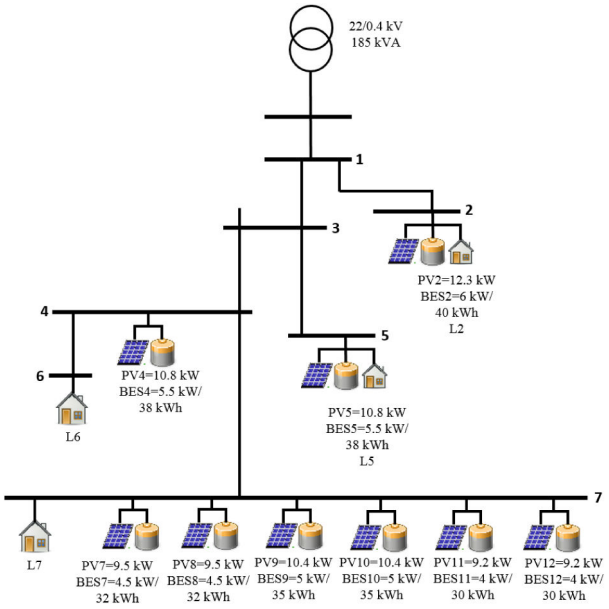

Fig. 4 *Diagram of test network*

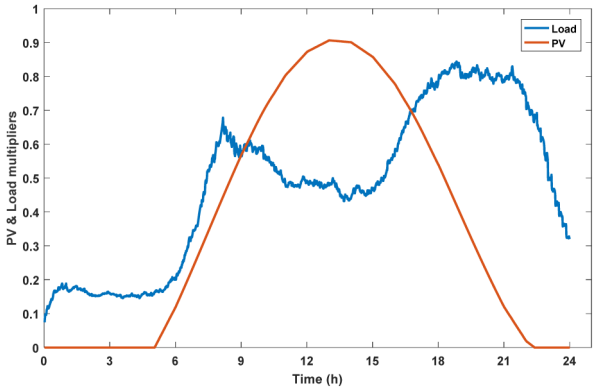

Fig. 5 *Load and demand profiles*

an active zone is not able to deal with events independently. BESSs in the active zone are added to $\mathrm{BES_{sel}}$, one at a time, depending on the severity of the event. The gradual addition of BESS in a zone to the $\mathrm{BES_{sel}}$ is similar to that seen in the FSSS. In other words, only the number of BESS required to make $V_{\mathrm{diff}} = 0$ at every bus in the zone are sequentially added to the $\mathrm{BES_{sel}}$. A unique feature of the RNPS is the use of a rotation array (RA) for charging and discharging operations in the zones. Each zone has two RAs; $\mathrm{RA_C}$ for charging operations and $\mathrm{RA_D}$ for discharging operations. The RA is the tool used by the RNPS to mitigate disproportionate cycling among BESS in any zone.

Each of $\mathrm{RA_C}$ and $\mathrm{RA_D}$ for each zone contains all the BESS in the zone, in the order to be followed for charging or discharging operations. The first BESS in $\mathrm{RA_C}$ and $\mathrm{RA_D}$ are the ones to respond to any charge or discharge signals, respectively, received at any bus in the zone. This is followed by the second BESS in the RAs when the first is unable to make $V_{\mathrm{diff}} = 0$, as a result of insufficient available capacity or persistence of distress signal despite charging or discharging at maximum rates. The third, then fourth and so on, are subsequently appointed following same rules. Once a BESS has been added to $\mathrm{BES_{sel}}$, the RA is updated with the same BESS moved from the first to the last position in the rank, while other BESSs move up one step in the rank. This sequence is the same for $\mathrm{RA_C}$ and $\mathrm{RA_D}$.

For example, $\mathrm{RA}_{C|B}$ is the rotation array for charging operations in zone B and contains the BESS in zone B, in the order in which they will respond to charge signals. On receipt of a charge signal on any bus in zone B, BESS_{B1} is added to B_{sel} and at the same time, moved to the last rank position in $\mathrm{RA}_{C|B}$, which is then updated as follows:

$$\mathrm{RA}_{C|B} = \begin{bmatrix} \mathrm{BES}_{B1} \\ \mathrm{BES}_{B4} \\ \mathrm{BES}_{B5} \\ \mathrm{BES}_{B2} \\ \mathrm{BES}_{B3} \end{bmatrix} \quad \text{to} \quad \begin{bmatrix} \mathrm{BES}_{B4} \\ \mathrm{BES}_{B5} \\ \mathrm{BES}_{B2} \\ \mathrm{BES}_{B3} \\ \mathrm{BES}_{B1} \end{bmatrix} \tag{17}$$

BESS_{B4} becomes the next BESS to respond to charge signal from zone B, and this happens when BESS_{B1} is fully charged or B1 is unable to bring $V_{\mathrm{diff}} = 0$ operating alone.

A similar sequence is maintained in $\mathrm{RA}_{D|B}$. Note that in $\mathrm{RA}_{D|B}$, the BESS can be ranked in an order different from $\mathrm{RA}_{C|B}$, but must contain the same BESS as $\mathrm{RA}_{C|B}$. The rotation of the BESS within the RA ensures that the charge/discharge responsibilities are evenly distributed among the participating BESS when assessed over a long period of time, such as during their entire lifetime.

6 Coordination algorithms implementation

This section describes the implementation of the three coordination algorithms presented in this work. The RNPS and UNPS are implemented on the same network while the FSSS is implemented on a different network.

6.1 Implementation of FSSS

The distribution network used as a case study in the implementation of the coordination scheme was developed using OpenDSS [9], an open-source tool developed by Electric Power Research Institute. The algorithm for the coordination control was developed in MATLAB. The Component Object Model (COM), which is made available in OpenDSS, was used as an interface to affect the controls on MATLAB to the network model on OpenDSS.

6.1.1 Case study network description: A 7-bus low-voltage radial distribution network [20], located in Belgium, was used for the implementation. four out of the seven buses (buses 2, 4, 5 and 7) have PV installed on them and the feeder is supplied through a 22/0.4 kV transformer rated 185 kVA. Thirty three residential houses are connected to the feeder and total kWp installation of PV on the feeder is 42.6 kWp. Six PV installations are on bus 7 while buses 2, 4, 5 contain single installations each, as shown in Fig. 4. The BESS on the network are named, as shown in Fig. 4, according to the buses to which they are connected. Multiple BESSs on bus 7 are numbered from 7 to 12.

6.1.2 Demand and generation profiles: The CREST tool [21] was used for the creation of the load profile used in the implementations. The tool was used to create load profiles for an aggregate of 100 houses, generating 50 different aggregations which were averaged out to obtain a typical representation of residential demand profile. The load shape was normalised and used as multipliers on the test network actual loads.

Summer-time load profile was generated to represent period of the year when PV generation is highest. This is shown in Fig. 5.

A generic summer-time PV profile representing average typical PV behaviour was used as the generation profile. Similar to the demand profile, the generation profile is applied as a multiplier to the actual kWp values of the PV installations on the test network. The resolution for both generation and demand profiles is 1 min.

6.1.3 Simulation results: Entire day simulations with a 1 min resolution were run to demonstrate the operations of the algorithm, giving a total simulation time of 1440 min. The following values were used for other parameter configurations of the scheme: $V_{\mathrm{UTH}} = 1.05\,\mathrm{p.u.}$, $V_{\mathrm{LTH}} = 0.98\,\mathrm{p.u.}$, $\mathrm{CR_{max.}} = 90\%$,

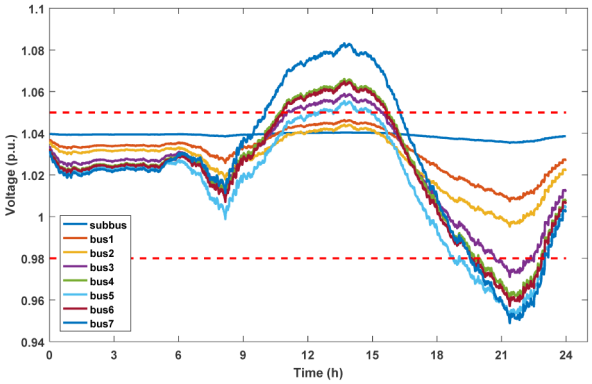

Fig. 6 *Feeder voltage profile without controls*

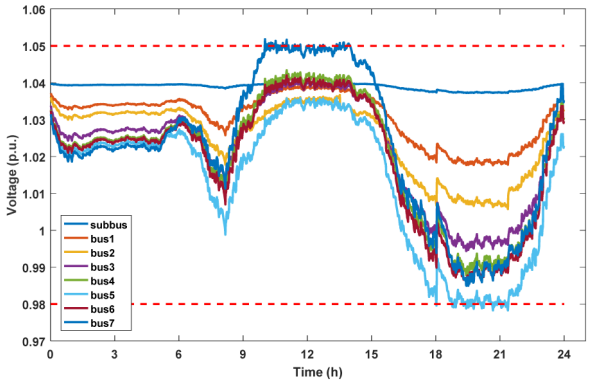

Fig. 7 *Feeder voltage profile with coordination control*

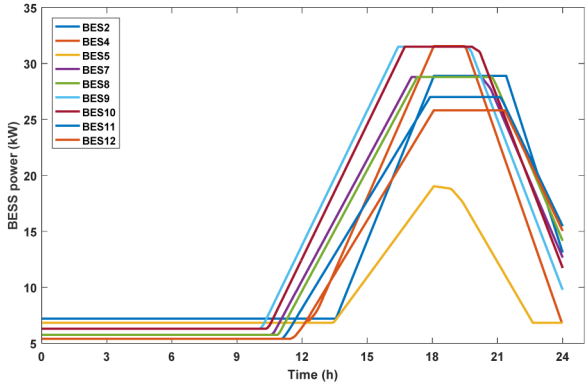

Fig. 8 *SOC of network BESS*

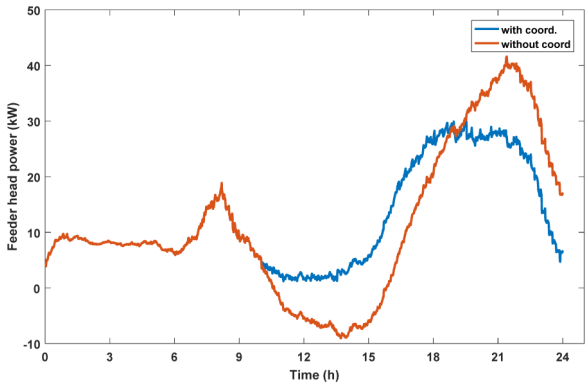

Fig. 9 *Power flows measured at the feeder head*

$20\% \leq \text{DOD} \leq 90\%$. The substation voltage was set at 1.04 p.u. in order to accommodate the voltage drop along the feeder.

The voltage profile of the network without any control scheme is shown in Fig. 6. It can be seen that both V_{UTH} and V_{LTH} are violated during periods of high PV generation and high demand, respectively. The former leads to curtailment of excess active power generated, which undermines the economics of PV installation. With the FSSS in operation, Fig. 7 shows the voltage profile of the feeder. At about the tenth hour, bus 7 experiences a voltage violation ($V_{m7} > V_{\text{UTH}}$) and BES_9 is switched to charging mode as it is the highest ranking on the SE. BES_{10} could also have been switched first since it has the same ranking as BES_9, given that they both have the same power ratings, availability according to Ω_{SOC} and are both positioned on the same bus. BES_{10} is switched to charging mode shortly after BES_9. This happens after CR_9 reaches CR_{max}, and $V_{\text{diff}} > 0$ still persists. With an increase in the PV generation, other BESSs are sequentially switched to charging mode and the FSSS also ensures there are no sudden voltage changes, especially when a BESS is fully charged or discharged. It accomplishes this by monitoring the updated Ω_{SOC} in order to keep track of the SOC of active BESS (Fig. 8).

In similar manner as in charging, discharge signals are sent to high ranking and available BESS during periods of heavy loading. In Fig. 7, $V_5 < V_{\text{LTH}}$ occurs around the 18th hour and BES_5 is the first to switch to discharge mode. Other BESSs are subsequently switched to discharge mode to ease loading on the network. Fig. 9 shows reverse power flow from the LV to MV network without the FSSS, which is mitigated by application of FSSS.

6.2 Implementation of UNPS

6.2.1 Case study network description: The hypothetical IEEE 33-bus distribution network [22] is used for the implementation of the UNPS and RNPS. The network was developed in OpenDSS while the algorithm implementation was built in Python. The COM interface of the OpenDSS was used for connecting Python to the OpenDSS model.

The substation voltage is 12.66 kV with total load demand of 3715 kW. Each bus of the network has PV installation of 70 kWp with co-located BESS of 50 kW/50 kWh. The network is shown in Fig. 3. Following the considerations described in Section 4.1, the network is segmented as shown in Fig. 3. The load and generation profiles created in Section 6.1 are used as multipliers on the actual loads and PV, respectively. The voltage at the feeder head is set at 1.05 p.u.

The BESSs are named both according to their operational zones and the bus number to which they are connected. The bus number follows the zone identifier in this naming convention. For example, the BESSs in zone A are named as follows: $[\text{BES}_{A13}, \text{BES}_{A14}, \text{BES}_{A15}, \text{BES}_{A16}, \text{BES}_{A17}, \text{BES}_{A18}]$. The zonal neighbourhood sets for zones A and B, which are the zones used for illustration of the scheme, are: $Z_{\text{nbr}|A} = [B, C, E]$ and $Z_{\text{nbr}A|B} = [A, C, E]$.

6.2.2 Simulation results of UNPS: Simulations were run for an entire day with 1 min resolution. The simulation was initialised with SOC = 100% for BES_{A18}, in order to capture variations that might be encountered in real operations where a BESS does not have capacity for charge prior to periods of high PV generation. Voltage profile of the network with UNPS in operation is shown in Fig. 10. Voltage violation ($V_{m18} > V_{\text{UTH}}$) occurs in zone A at about the 12th hour at bus 18 and the zone is switched to charge mode. The BESSs in zone A charge uniformly, with charge rates determined by the magnitude of V_{diff} on the overvoltage bus. Fig. 11 shows the SOC of the BESSs in zones A and B. The SOC for each zone can be seen varying uniformly throughout the duration of the simulation. In the evening during periods of high loading on the network, the BESSs are switched to discharge mode. Around the 22nd hour, zone A BESSs become fully charged, even though there is still need for maintaining the voltages in zone A within the set range. The algorithm, at this stage, uses $Z_{\text{nbr}|A}$, (the zonal neighbourhood set for zone A) to appoint a neighbour zone that switches into operation for the purpose of maintaining voltages. Zone B is the first element in Z_{nbr} and is appointed. As seen in Fig. 11, zone B BESSs (BES_{B10}, BES_{B11}, BES_{B12}) start

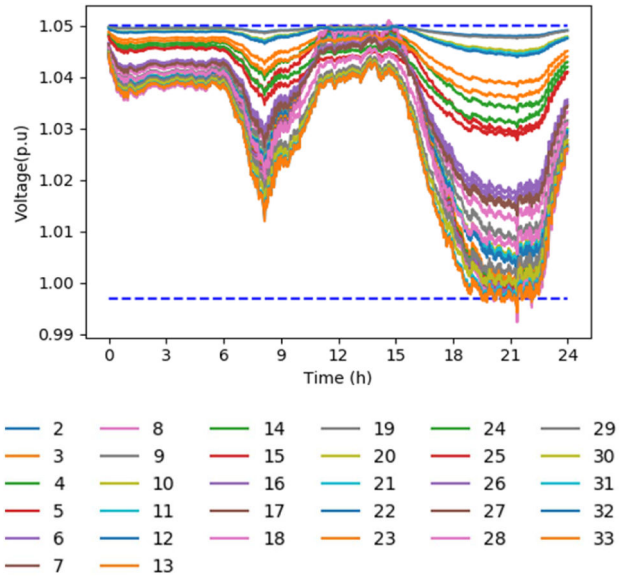

Fig. 10 *Feeder voltage profile with UNPS*

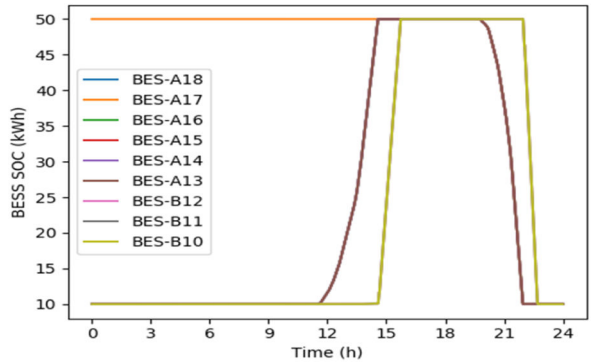

Fig. 11 *SOC of zone A with UNPS*

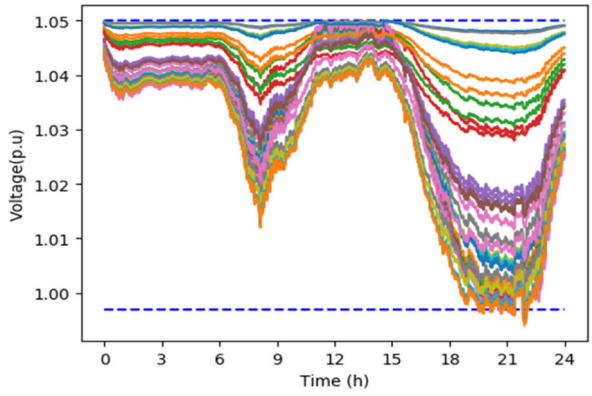

Fig. 12 *Feeder voltage profile with RNPS*

discharging at about the same time that zone A BESSs become fully charged (around the 22nd hour).

6.3 Implementation of RNPS

The same network, zone segmentation, load and generation profiles used in Section 6.2 are also used in this section for the demonstration of the operations of the RNPS. To demonstrate the rotational sequencing of the BESSs using the RNPS, zone A will be focused on for simplicity. Behaviours in other zones of the network will be similar to zone A's. The initial RAs for zone A are given below:

$$\mathrm{RA}_{\mathrm{C}|A} = \begin{bmatrix} \mathrm{BES}_{A18} \\ \mathrm{BES}_{A17} \\ \mathrm{BES}_{A16} \\ \mathrm{BES}_{A15} \\ \mathrm{BES}_{A14} \\ \mathrm{BES}_{A13} \end{bmatrix}, \quad \mathrm{RA}_{\mathrm{D}|A} = \begin{bmatrix} \mathrm{BES}_{A17} \\ \mathrm{BES}_{A18} \\ \mathrm{BES}_{A16} \\ \mathrm{BES}_{A15} \\ \mathrm{BES}_{A14} \\ \mathrm{BES}_{A13} \end{bmatrix} \tag{18}$$

The initial SOC values of the BESS in zone A are 20% (minimum SOC), except BES_{A17} which starts at 100%.

6.3.1 Simulation results of RNPS: Fig. 12 shows the voltage profile of the feeder with the RNPS in operation.

As PV power generation increases, bus 18 at the end of the feeder is the first to have its voltage exceed the upper threshold ($V_{m18} > V_{\mathrm{UTH}}$) around the 12th hour. BES_{A18} is switched to charge mode, being the top ranked in $\mathrm{RA}_{\mathrm{C}|A}$.

Fig. 13 shows how the orders of the BESSs are changing as their SOC change. A zoomed-in view is presented in Fig. 14 for clearer details. The magnified area is indicated by the block dotted oval on Fig. 13. The legend and colour schemes are the same as those used in Fig. 11. When BES_{A18} reaches maximum SOC, it is moved to the bottom of $\mathrm{RA}_{\mathrm{C}|A}$ and other BESSs in the set move up one step. The new highest-ranked BESS becomes BES_{A16} because the algorithm detects that BESS_{A17} is fully charged (from initial settings), moves it to the bottom of the set and makes BES_{A16} the priority for charging. The BESSs are brought to charge sequentially according to the ranking in $\mathrm{RA}_{\mathrm{C}|A}$ until a signal for discharge is received around the 20th hour. BESS_{17}, being the highest-ranked in $\mathrm{RA}_{\mathrm{D}|A}$ is the first to start discharging. The other BESSs in the zone follow according to their positions on $\mathrm{RA}_{\mathrm{D}|A}$.

Around the 14th hour, a situation arises where all the BESSs in zone A are either fully charged, or charging at maximum rates but not able to mitigate the distress signal. The algorithm uses the Z_{nbr} of zone A, which has zone B as the first element, to solve the problem. BES_{B12} is switched to charging, followed by BES_{B11}. The voltage along the feeder is maintained during the period of high PV generation and high network loading. Two possible objectives could be set as target for the BESS discharge – a power threshold at the secondary of the substation or undervoltage at the buses. The latter has been used in this simulation and was set at 0.999 V p . u.

7 Conclusion and future work

In this paper, three different schemes for the coordination of multiple BESSs in a network were proposed. The schemes in operation mitigated the occurrence of overvoltage as a result of high PV generation on the network. During peak loading times on the network, the BESSs on the network were also coordinated to support the network. Voltage sensitivity was used for selection and charge rates estimation for the FSSS. Segmentation of the network into BESS operational zones was performed in the UNPS and the RNPS to ensure more efficient and even cycling of the BESS on the network. Simulations were carried out using two different networks to demonstrate the performance of the schemes and results show that the schemes were able to mitigate overvoltage and that different schemes could be applied to different networks depending on specific network structure and techno-economic objectives. The schemes presented in this paper can be employed by utilities and owners of BESS to improve the lifetime of BESS while maximising the penetration of renewable energy resources in the network without technical challenges.

Future research will consider the implementation of the schemes on different networks and carrying out simulations to compare the performance of the schemes with other earlier-developed schemes in literature. In addition, the performance of the schemes in managing the lives of the BESS will be evaluated individually by carrying out simulations for the entire lifetimes of the BESS.

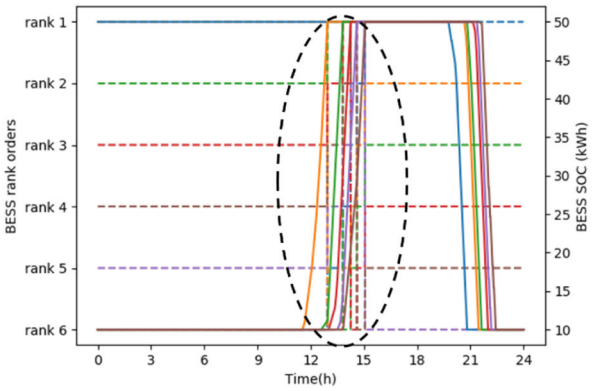

Fig. 13 *Rotational order and SOC at zone A*

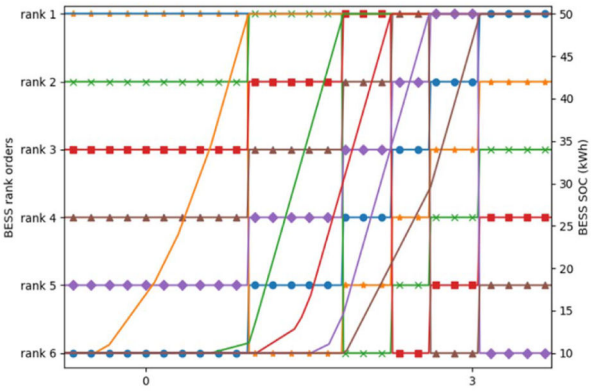

Fig. 14 *Zoomed-in rotational order and SOC at zone A*

8 Acknowledgment

The authors acknowledge the support by the following: (i) Petroleum Technology Development Fund (PTDF), an initiative of the Federal Government of Nigeria; (ii) The British Council UK – India Education & Research Initiative & the Indian Department of Science & Technology under grant 16/17-98 (D-DIEM: Data-Driven Intelligent Energy Management for Environmentally Sustainable Energy Access); (iii) EPSRC through the National Centre for Energy Systems Integration, grant number EP/P001173/1.

9 References

[1] Jäger-Waldau, A.: 'European commission PV status report 2017'. Publications Office of the European Union, Luxembourg, 2017

[2] Pereira, B.R., Martins Da Costa, G.R.M., Contreras, J., *et al.*: 'Optimal distributed generation and reactive power allocation in electrical distribution systems', *IEEE Trans. Sustain. Energy*, 2016, **7**, (3), pp. 975–984

[3] Min, S.W., Kim, S.-J., Shim, J.W., *et al.*: 'Synergistic control of SMES and battery energy storage for enabling dispatchability of renewable energy sources', *IEEE Trans. Appl. Supercond.*, 2013, **23**, (3), pp. 5701205–5701205

[4] Nykvist, B., Nilsson, M.: 'Rapidly falling costs of battery packs for electric vehicles', *Nat. Clim. Chang.*, 2015, **5**, (4), pp. 329–332

[5] Schmidt, O., Hawkes, A., Gambhir, A., *et al.*: 'The future cost of electrical energy storage based on experience rates', *Nat. Energy*, 2017, **2**, (8), p. 17110

[6] Manwell, J.F., Rogers, A., Hayman, G., *et al.*: 'Hybrid2 – a hybrid system simulation model theory manual', Natl. Renew. Energy Lab., 2006

[7] Alam, M.J.E., Muttaqi, K.M., Sutanto, D.: 'Mitigation of rooftop solar PV impacts and evening peak support by managing available capacity of distributed energy storage systems', *IEEE Trans. Power Syst.*, 2013, **28**, (4), pp. 3874–3884

[8] Jayasekara, N., Masoum, M.A.S., Wolfs, P.J.: 'Optimal operation of distributed energy storage systems to improve distribution network load and generation hosting capability', *IEEE Trans. Sustain. Energy*, 2016, **7**, (1), pp. 250–261

[9] Unigwe, O., Okekunle, D., Kiprakis, A.: 'Economical distributed voltage control in low-voltage grids with high penetration of photovoltaic', *CIRED – Open Access Proc. J.*, 2017, **2017**, (1), pp. 1722–1725

[10] Ranaweera, I., Midtgård, O.-M., Korpås, M.: 'Distributed control scheme for residential battery energy storage units coupled with PV systems'

[11] Nguyen, M.Y., Nguyen, D.H., Yoon, Y.T.: 'A new battery energy storage charging/discharging scheme for wind power producers in real-time markets', *Energies*, 2012, **5**, (12), pp. 5439–5452

[12] Lee, S.-J., Kim, J.-H., Kim, C.-H., *et al.*: 'Coordinated control algorithm for distributed battery energy storage systems for mitigating voltage and frequency deviations', *IEEE Trans. Smart Grid*, 2016, **7**, (3), pp. 1713–1722

[13] Wang, L., Liang, D.H., Crossland, A.F., *et al.*: 'Coordination of multiple energy storage units in a low-voltage distribution network', *IEEE Trans. Smart Grid*, 2015, **6**, (6), pp. 2906–2918

[14] Abdullah, M.A., Muttaqi, K.M., Sutanto, D., *et al.*: 'An effective power dispatch control strategy to improve generation schedulability and supply reliability of a wind farm using a battery energy storage system', *IEEE Trans. Sustain. Energy*, 2015, **6**, (3), pp. 1093–1102

[15] Unigwe, O., Okekunle, D., Kiprakis, A.: 'Smart coordination of battery energy storage systems for voltage control in distribution networks with high penetration of photovoltaics', pp. 1–6

[16] Tonkoski, R., Turcotte, D., El-Fouly, T.H.M.: 'Impact of high PV penetration on voltage profiles in residential neighborhoods', *IEEE Trans. Sustain. Energy*, 2012, **3**, (3), pp. 518–527

[17] 'IEEE standard for interconnecting distributed resources with electric power systems', IEEE Std 1547-2003, no. August, 2003, pp. 1–122

[18] Teo, T.T., Logenthiran, T., Woo, W.L., *et al.*: 'Advanced control strategy for an energy storage system in a grid-connected microgrid with renewable energy generation', *IET Smart Grid*, 2018, **1**, (3), pp. 96–103

[19] Brenna, M., De Berardinis, E., Carpini, L.D., *et al.*: 'Automatic distributed voltage control algorithm in smart grids applications', *IEEE Trans. Smart Grid*, 2013, **4**, (2), pp. 877–885

[20] Zeraati, M., Hamedani Golshan, M.E., Guerrero, J.: 'Distributed control of battery energy storage systems for voltage regulation in distribution networks with high PV penetration', *IEEE Trans. Smart Grid*, 2016, **9**, (4), pp. 3582–3593

[21] McKenna, E., Thomson, M.: 'High-resolution stochastic integrated thermal–electrical domestic demand model', *Appl. Energy*, 2016, **165**, pp. 445–461

[22] Venkatesh, B., Ranjan, R., Gooi, H.B., *et al.*: 'Optimal reconfiguration of radial distribution systems to maximize loadability', *IEEE Trans. Power Syst.*, 2004, **19**, (1), pp. 260–266